Atti Accademia Nazionale dei Lincei

Classe Scienze Fisiche Matematiche Naturali

Rendiconti

Michele Caputo, Rodolfo Console

Seismic inversion for a crak opening

Atti della Accademia Nazionale dei Lincei. Classe di Scienze Fisiche, Matematiche e Naturali. Rendiconti, Serie 8, Vol. **82** (1988), n.4, p. 757–771.

Accademia Nazionale dei Lincei

<http://www.bdim.eu/item?id=RLINA_1988_8_82_4_757_0>

Atti della Accademia Nazionale dei Lincei. Classe di Scienze Fisiche, Matematiche e Naturali. Rendiconti, Accademia Nazionale dei Lincei, 1988.

Atti Acc. Lincei Rend. fis.
(8), LXXXII (1988), pp. 757-771

Sismologia. — *Seismic inversion for a crak opening.* Nota di Michele Caputo (*) e Rodolfo Console (**), presentata (***) dal Socio M. Caputo.

Abstract. — The displacement field caused by the classic earthquake mechanism model consisting of a slip along the fault is extended to the case when besides the slip, also an opening occurs caused by tensional forces. The tensor matrix describing the moment tensor does not necessarily have a nil trace. The direct problem is solved finding the radiation pattern for P and S waves.

A method to solve the inverse problem of the determination of the four parameters describing the source is presented and tested on data produced with the solution of the direct problem. The tests suggest that the method is valid depending on the accuracy of the data, the distribution of observing stations and ratio of the opening to the slip components as expected. It would give good results with the modern instrumentation and the most common distribution of stations.

Key words: Focal mechanism; Crack opening; Radiation pattern.

Riassunto. — *Determinazione della formazione (e giacitura) di fratture da dati sismologici.* In questo lavoro viene presentata un'estensione del modello che descrive una sorgente sismica come una pura dislocazione di taglio, introducendo un'apertura della faglia causata da forze tensionali. La sorgente sismica viene così caratterizzata, oltre che da i tre parametri classici di una faglia, anche da un quarto parametro, identificabile nell'angolo (non nullo) compreso tra il piano della faglia ed il vettore della dislocazione. La descrizione matematica del modello prevede che la matrice del tensore dei momenti non abbia necessariamente una traccia di valore nullo.

Per tale tipo di sorgente il problema diretto viene risolto ricavando la funzione di irraggiamento per le onde P e per le onde S. Viene poi proposto un metodo per la determinazione dei quattro parametri del modello in una sorgente reale, a partire dalle ampiezze osservate delle onde P.

Il metodo è stato sottoposto a verifiche numeriche nelle quali i dati, compredenti anche errori sperimentali sono stati generati sinteticamente dalle formule sviluppate con la soluzione del problema diretto. Tali verifiche dimostrano che dati di ragionevole precisione possono consentire la discriminazione di una sorgente contenente un'apertura da una caratterizzata da pura dislocazione di taglio.

Introduction

The determination of the earthquake source mechanism is one of the fundamental problems in seismology; in recent decades the problem has attracted the attention of many researchers and recently with the introduction of the moment tensor formulation great progress has been made.

Gilbert (1971) proposed a method for determining the source mechanism without referring to a specific model. The method was used for free oscillations by Gilbert and Dziewonsky (1975), for surface waves by McCowan (1976) and Mendiguren (1977) and for body waves by Stump (1976).

In the case of an earthquake caused by a dislocation on a fault with additional opening of the fault caused by tension forces the sources must contain tensional forces

(*) Dipartimento di Fisica «G. Marconi», Università degli Studi di Roma.
(**) Istituto Nazionale di Geofisica, Roma.
(***) Nella seduta del 12 dicembre 1987.

acting normally to the surface of the fault. The opening of the fault naturally causes a contraction, generally with revolution symmetry around an axis normal to the fault, which implies that the moment tensor has only five free parameters. Assuming for this type of source a generic moment tensor with six free parameters, since the solution «prefers» the model with the largest number of free parameters due to the observational errors, one would find a source with features due to error fitting and not necessarily having physical reality. In the case of fault opening, one should try a seismic moment model with the above mentioned axial symmetry. If there is still doubt about this symmetry, the model with six free parameters may also be tried; a χ^2 test could possibly be used to decide which of the solutions was more reliable.

De Natale and Zollo (1986) considered the method based on the signs and the amplitudes of the first arrival of the seismic signals. They used two different source models: the first in which the trace of the moment tensor matrix is nil and the secondo with six unrestrained parameters.

In this paper we shall introduce a method which is also based on the signs and the amplitudes of the first arrival of the seismic signals at the different recording stations. In our method the trace of the moment tensor is allowed to be different from zero with the limitation that there be symmetry of revolution around the axis normal to the fault in the stress field represented by the diagonal elements of the stress tensor. The limitation due to the required symmetry of revolution is recommended especially in the seismic regions subject to tension, such as back arc, volcanic and, perhaps, geothermal regions. Seismic events occurring in tensional regions are sometimes interpreted as the interaction of pressurizing fluid with opening cracks. In these case their focal mechanism should be characterized by significant non-double-couple components, as really observed for volcanic earthquakes (Julian and Sipkin, 1985). The observation of such mechanisms could therefore be useful for investigation about the behaviour of the rock-water system in geothermal fields.

We shall first solve the direct problem of the determination of the Green function extending the classic procedure of the double couple of forces acting parallel to the plane of the fault (Aki and Richards, 1980) to the more general case where there is also a normal component of stress, perpendicular to the fault faces. In terms of dislocation we could figuratively say that this is not in the plane of the fault but, with the slip parallel to the fault, there is also an opening of the fault itself.

In order to solve the inverse problem, we shall rearrange the formulas obtained with the solution of the direct problem, having corrected them for the ray paths in the assumed crustal model. The method used here was developed by Shapira and Bath (1978) for a pure shear source. It is based on the trial and error technique, iteratively changing the source parameters to minimize the differences between the amplitudes observed at the stations and those computed.

The solution of the direct problem.

The n component of the displacement $\boldsymbol{u}$ in P caused by a point source, in the origin of the coordinates, with moment tensor M_{pq} is obtained (e.g. Aki and Richards,

1980) from the convolution

(1) $$u_n = M_{qp} * G_{nq,p}$$

where G_{nq} is the Green function for a point force in the direction of the axis x_x. M_{qp} are the components of the moment tensor

(2) $$M_{pq} = \iint_{\Sigma} m_{pq}\, d\Sigma = \iint_{\Sigma} (\lambda \nu_k [u_k] \delta_{pq} + \mu[\nu_p u_q + \nu_q u_p])\, d\Sigma,$$

where m_{pq} is the moment tensor density, ν_k are the components of the normal to the surface Σ where the dislocation occurred, λ and μ are the elastic parameters and $[u_i]$ are the components of the dislocation on Σ.

For the far field the Green function may be written explicitly and from (1) we obtain

(3) $$u_n = \frac{\gamma_n \gamma_p \gamma_q}{4\pi\rho\alpha^3 r} \dot{M}_{pq}\left(t - \frac{r}{\alpha}\right) - \frac{(\gamma_n \gamma_p - \delta_{np})\gamma_q}{4\pi\rho\beta^3 r} \dot{M}_{pq}\left(t - \frac{r}{\beta}\right),$$

where γ_i are components of the unit vector in the direction from the source to the receiver separated by the distance r in the homogeneous medium, α and β are the velocities of the P and S waves. Explicitly, for a elementary fault of area A, we may write

(4) $$u_n = \frac{A}{4\pi\rho\alpha^3 r}[\lambda \gamma_n \nu_k \dot{u}_k + 2\mu \gamma_n \gamma_p \gamma_q \nu_q \dot{u}_p] + \\ - \frac{\mu A}{4\pi\rho\beta^3 r}[2\gamma_n \gamma_q \nu_q \gamma_p \dot{u}_p - \gamma_p \nu_n \dot{u}_p - \delta_{np} \gamma_q \nu_q \dot{u}_p],$$

where the first expression in square brackets is computed at the delayed time $t - r/\alpha$ and the second at the time $t - r/\beta$.

Let us now transfer the components of u, which are in the x_1, x_2, x_3 system of the source into the $\hat{r}$, $\hat{\vartheta}$, $\hat{\varphi}$ coordinate system of the station in P defined as shown in the figure where $\hat{\vartheta}$ is perpendicular to $\hat{r}$ and in the plane OPQ, positive from $\hat{x}_3$; $\hat{\varphi}$ is perpen-

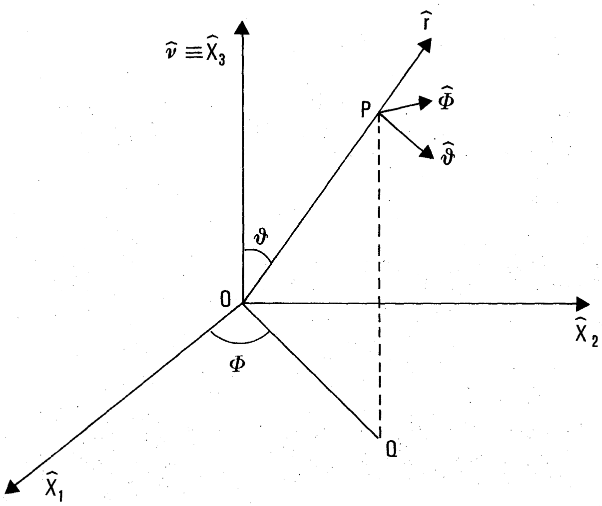

Fig. 1. – Coordinate systems used to determine the radiation patt.

dicular to $\hat{r}$ and $\hat{\vartheta}$, positive counterclockwise; the fault is in O and in the plane x_1, x_2; the slip $\boldsymbol{u}$ may not be in the plane of the fault; we shall take it in the most general direction, rotating the reference frame around $\hat{x}_3$ to contain it in the plane $x_1\ x_3 : \boldsymbol{u} = u_1\ \hat{x}_1 + u_3\ \hat{x}_3$.

According to the figure we obtain the components of $\hat{\gamma} = \hat{r}$, $\hat{\vartheta}$ and $\hat{\varphi}$ in the x_1, x_2 x_3 system

$$\tag{5} \begin{cases} \hat{\gamma} = \hat{r} = \sin\vartheta\cos\varphi\hat{x}_1 + \sin\vartheta\sin\varphi\hat{x}_2 + \cos\vartheta\hat{x}_3\,, \\ \hat{\vartheta} = \cos\vartheta\cos\varphi\hat{x}_1 + \cos\vartheta\sin\varphi\hat{x}_2 - \sin\vartheta\hat{x}_3\,, \\ \hat{\varphi} = -\sin\varphi\hat{x}_1 + \cos\varphi\hat{x}_2\,, \end{cases}$$

we obtain also the components of $\hat{x}_1$; in the $\hat{r}$, $\hat{\vartheta}$, $\hat{\varphi}$ system of the station

$$\tag{6} \begin{cases} \hat{x}_1 = \sin\vartheta\cos\varphi\hat{r} + \cos\vartheta\cos\varphi\hat{\vartheta} - \sin\varphi\hat{\varphi}, \\ \hat{x}_3 = \cos\vartheta\hat{r} + \sin\vartheta\hat{\vartheta}, \\ \overline{u} = (u_1\sin\vartheta\cos\varphi + u_3\cos\vartheta)\hat{r} + (u_1\cos\vartheta\cos\varphi + u_3\sin\vartheta)\hat{\vartheta}, \end{cases}$$

The four types of products appearing in (4) may be now expressed in terms of $\hat{r}$, $\hat{\vartheta}$, $\hat{\varphi}$, considering first that the dot product is independent of coordinates

$$\tag{7} \begin{cases} \nu_k u_k = u_3\,, \\ \nu_k \gamma_k = x_3\gamma_3 = \cos\vartheta, \\ \gamma_k u_k = \gamma_1 u_1 + \gamma_3 u_3 = u_1\sin\vartheta\cos\varphi + u_3\cos\varphi, \\ (\gamma_r\nu_r)(\gamma_k u_k) = u_1\sin\vartheta\cos\vartheta\cos\varphi + u_3\cos^2\vartheta, \end{cases}$$

then

$$\tag{8} \begin{aligned} &\gamma_n(\nu_k\dot{u}_k) = \dot{u}_3\hat{r} + 0\hat{\vartheta} + 0\hat{\varphi}, \quad \text{because} \quad \hat{\gamma} \equiv \hat{r}, \\ &\gamma_n(\nu_k\gamma_k)(\gamma_r\dot{u}_r) = \cos\vartheta(u_1\sin\vartheta\cos\varphi + u_3\cos\vartheta)\hat{r}, \\ &\nu_n(\gamma_k\dot{u}_k) = (\dot{u}_1\sin\vartheta\cos\varphi + \dot{u}_3\cos\vartheta)(\cos\vartheta\hat{r} - \sin\vartheta\hat{\vartheta}), \\ &\delta_{np}(\gamma_q\nu_q)\dot{u}_p = (\gamma_q\nu_q)\dot{u}_n = \\ &= \cos\vartheta[(\dot{u}_1\sin\vartheta\cos\varphi + \dot{u}_3\cos\varphi)\hat{r} + (\dot{u}_1\cos\vartheta\cos\varphi + \dot{u}_3\sin\vartheta)\hat{\vartheta} + \dot{u}_1\sin\varphi\hat{\varphi}], \end{aligned}$$

to be substituted in (4) to obtain the components of the displacement in the $\hat{r}$, $\hat{\vartheta}$, $\hat{\varphi}$ system of the station.

The only nonzero component due to the P wave at station is in the r direction; it is

$$\tag{9} \frac{\mu A}{4\pi\rho\alpha^3 r}\left[\frac{\lambda}{\mu}\dot{u}_3 + 2(\dot{u}_1\sin\vartheta\cos\varphi + \dot{u}_3\cos\vartheta)\cos\vartheta\right]\hat{r}.$$

While the non nil components due to the S wave at station are

$$\tag{10} \frac{\mu A}{4\pi\rho\alpha^3 r}\,[(\dot{u}_1\cos\varphi\ \cos 2\vartheta)\hat{\vartheta} - \dot{u}_1\cos\vartheta\sin\varphi\hat{\varphi}].$$

The $\hat{r}$ component due the S wave is nil, and the $\hat{\vartheta}$ and $\hat{\varphi}$ components give the S radiation pattern.

In order to be able to use the formulas obtained above, we shall express them as

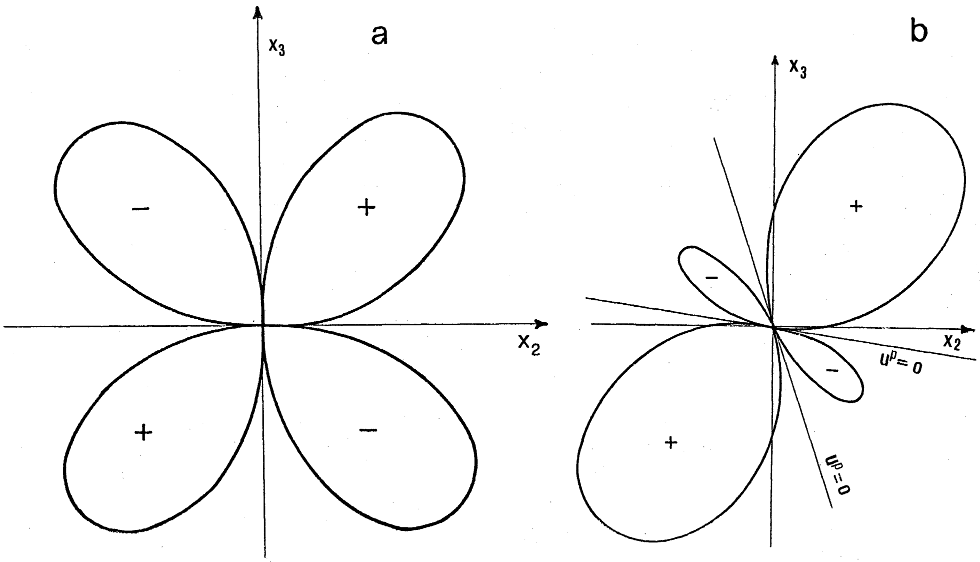

Fig. 2. – Radiation pattern for (*a*) a pure shear source and for (*b*) a source with a component of dislocation normal to the fault plane ($u_3 = 0.2\, u_1$).

functions of the angles describing the directions of source plane and of the slip, which are the unknowns of the problem to be estimated from the recording of the signals at the stations around the source. For this purpose let us write (4) in vector form where u is the vector representing the dislocation

$$
(11) \qquad \begin{cases} \boldsymbol{u}^P = \dfrac{\dfrac{\lambda}{\mu}(\dot{\boldsymbol{u}}\cdot\hat{\nu}) + 2(\hat{\gamma}\cdot\hat{\nu})(\hat{\gamma}\cdot\dot{\boldsymbol{u}})}{4\pi\rho\alpha^3 r}\,\mu A\hat{\gamma} = \mathcal{F}^P\,\dfrac{\mu A}{4\pi\rho\alpha^3 r}\,\hat{l}\,|\dot{\boldsymbol{u}}|\,, \\[2ex] \boldsymbol{u}^S = \dfrac{(\hat{\gamma}\cdot\hat{\nu})\,\dot{\boldsymbol{u}} + (\hat{\gamma}\cdot\dot{\boldsymbol{u}})\,\hat{\nu}/ - 2(\hat{\gamma}\cdot\hat{\nu})(\hat{\gamma}\cdot\dot{\boldsymbol{u}})\,\hat{\gamma}}{4\pi\rho\beta^3 r}\,\mu A\,, \end{cases}
$$

where $\boldsymbol{u}^P$ is computed at $t - r/\alpha$ and $\boldsymbol{u}^s$ at $t - r/\beta$.

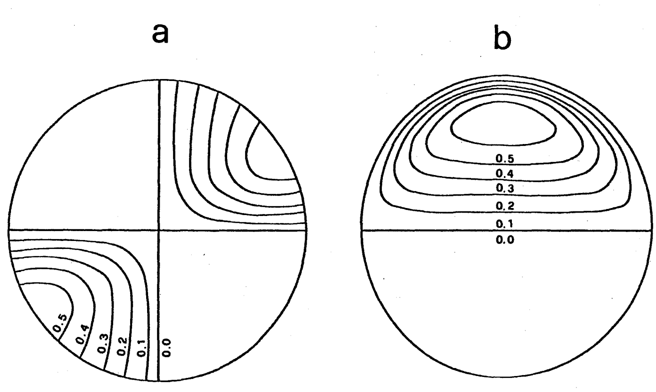

Fig. 3. – Nodal lines in the lower hemisphere projection for (*a*) a dip slip fault and for (*b*) a strike slip fault, shown for different values of the dislocation component normal to the fault plane.

As before

$\hat{\nu}$ is the unit vector of the normal to the fault,

$\hat{\gamma}$ is the unit vector directed from the source to the receiver,

$\hat{l}$ is the unit vector in direction of the ray ($\hat{l} \equiv \hat{\gamma}$),

$\hat{p}$ is the unit vector perpendicular to $\hat{l}$ in the vertical plane through $\hat{l}$, positive upwards;

$\hat{\varphi}$ is the unit vector perpendicular to $\hat{l}$ and to $\hat{p}$ in the horizontal plane.

We obtain then $\boldsymbol{u}^{SH}$ and $\boldsymbol{u}^{SV}$ from the second formula of (11):

$$\boldsymbol{u}^{SH} = (\boldsymbol{u}^S \cdot \hat{\varphi})\,\hat{\varphi} = \frac{(\hat{\gamma}\cdot\hat{\nu})(\dot{\boldsymbol{u}}\cdot\hat{\varphi}) + (\hat{\gamma}\cdot\dot{\boldsymbol{u}})(\hat{\nu}\cdot\hat{\varphi})}{4\pi\rho\beta^3 r}\mu A\hat{\varphi} = \mathcal{F}^{SH}\frac{\mu A}{4\pi\rho\beta^3 r}\hat{\varphi}|\dot{\boldsymbol{u}}|, \tag{12}$$

$$\boldsymbol{u}^{SV} = (\boldsymbol{u}^S \cdot \hat{p})\,\hat{p} = \frac{(\hat{\gamma}\cdot\hat{\nu})(\dot{\boldsymbol{u}}\cdot\hat{p}) + (\hat{\gamma}\cdot\dot{\boldsymbol{u}})(\hat{\nu}\cdot\hat{p})}{4\pi\rho\beta^3 r}\mu A\hat{p} = \mathcal{F}^{SV}\frac{\mu A}{4\pi\rho\beta^3 r}\hat{p}|\dot{\boldsymbol{u}}|. \tag{13}$$

Let us now consider an orthogonal cartesian reference frame with the origin on the surface of the Earth, the z axis vertical, containing the source and positive downward, the x axis pointing to North and the y axis toward East as shown in the figure.

Let us also assume that the dislocation vector $\boldsymbol{u}$ has a component $\boldsymbol{u}_t$ in the plane of the fault and a component $\boldsymbol{u}_n$ normal to it. We must now formulate $\boldsymbol{u}$, $\hat{\nu}$, $\hat{l}$, $\hat{p}$, $\hat{\varphi}$, in the new coordinate system. Let us indicate with $QQ_1 = u_t \cos\lambda$ the component of $\boldsymbol{u}_t$ on the horizontal straight line of the fault plane with $QQ_2 = u_t \sin\lambda$ the component of $\boldsymbol{u}_t$ on the straight line of the fault with maximum slope.

The component of QQ_2 on xy is another horizontal component of $\boldsymbol{u}_t$; it is $QQ_2 \cos\delta = u_t \sin\lambda \cos\delta$. The component of $\boldsymbol{u}_t$ along z is $u_t \sin\lambda \sin\delta$.

We may now compute the x and y components of the two independent horizontal

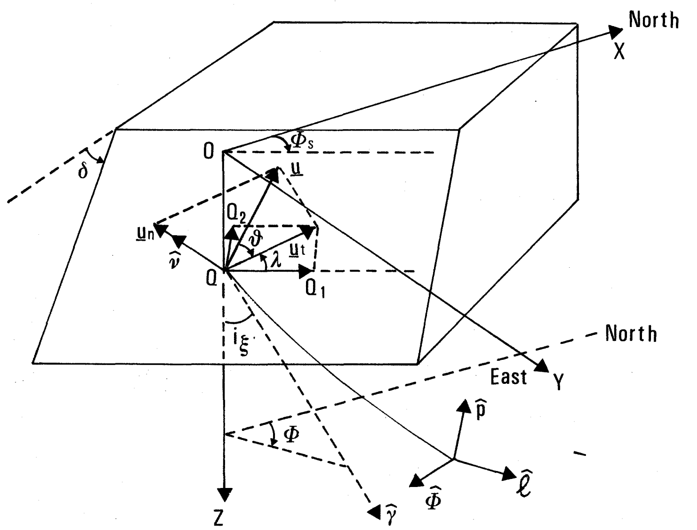

Fig. 4. – Coordinate systems and components of the displacement vectors used to solve the direct problem.

components: $u_t \cos\lambda$ and $u_t \sin\lambda \cos\delta$. By projecting them on x and y, we find

$$\left\{\begin{array}{ll} \text{on } x: & \cos\lambda\cos\varphi_S + \cos\delta\sin\lambda\sin\varphi_S\,, \\ \text{on } y: & \cos\lambda\sin\varphi_S - \cos\delta\sin\lambda\cos\varphi_S\,. \end{array}\right. \tag{14}$$

Finally we obtain for the displacement vector $\boldsymbol{u}_t$ the following expression

$$\boldsymbol{u}_t = u_t(\cos\lambda\cos\varphi_S + \cos\delta\sin\lambda\sin\varphi_S)\hat{x} + \\ + u_t(\cos\lambda\sin\varphi_S - \cos\delta\sin\lambda\cos\varphi_S)\hat{y} - u_t\sin\lambda\sin\delta\hat{z}, \tag{15}$$

or, considering that the horizontal component of $\hat{\nu}$ is $-\sin\delta$ and the vertical one is $-\cos\delta$

$$\left\{\begin{array}{l} \hat{\nu} = -\sin\delta\sin\varphi_S\,\hat{x} + \sin\delta\cos\varphi_S\,\hat{y} - \cos\delta\hat{z}, \\ \boldsymbol{u} = \boldsymbol{u}_t + \boldsymbol{u}_n \qquad \boldsymbol{u}_n = u_n\,\hat{\nu}, \\ \boldsymbol{u} = [u_t(\cos\lambda\cos\varphi_S + \cos\delta\sin\lambda\sin\varphi_S) - u_n\sin\delta\sin\varphi_S]\hat{x} + [u_t(\cos\lambda\sin\varphi_S - \\ \qquad -\cos\delta\sin\lambda\cos\varphi_S) + u_n\sin\delta\cos\varphi_S]\hat{y} - [u_t\sin\lambda\sin\delta + u_n\cos\delta]\hat{z}. \end{array}\right. \tag{16}$$

We may now go back to the second of (11), (12) and (13), and substitute $\boldsymbol{u} = \boldsymbol{u}_t + \boldsymbol{u}_n$.

In order to obtain a result in terms of i_ξ, φ, λ, δ, φ_S where λ, δ, φ_S are unknown and φ, i_ξ are known, let us note that

$$\left\{\begin{array}{lll} P & \text{wave} & \hat{l} = \hat{\gamma} = \sin i_\xi\cos\varphi\hat{x} + \sin i_\xi\sin\varphi\hat{y} + \cos i_\xi\,\hat{z}, \\ SV & \text{wave} & \hat{p} = \cos i_\xi\cos\varphi\hat{x} + \cos i_\xi\sin\varphi\hat{y} - \sin i_\xi\,\hat{z}, \\ SH & \text{wave} & \hat{\varphi} = -\sin\varphi\hat{x} + \cos\varphi\hat{y}, \end{array}\right. \tag{17}$$

which allow to compute the products of (11), (12) and (13)

$$\left\{\begin{array}{l} P \quad \text{wave} \quad (\hat{\gamma}\cdot\hat{\nu})(\hat{\gamma}\cdot\dot{\boldsymbol{u}})/|\dot{\boldsymbol{u}}|, \\ SV \quad \text{wave} \quad [(\hat{\gamma}\cdot\hat{\nu})(\dot{\boldsymbol{u}}\cdot\hat{p}) + (\hat{\gamma}\cdot\dot{\boldsymbol{u}})(\hat{\nu}\cdot\hat{p})]/|\dot{\boldsymbol{u}}|, \\ SH \quad \text{wave} \quad [(\hat{\gamma}\cdot\hat{\nu})(\dot{\boldsymbol{u}}\cdot\hat{\varphi}) + (\hat{\gamma}\cdot\dot{\boldsymbol{u}})(\hat{\nu}\cdot\hat{\varphi})]/|\dot{\boldsymbol{u}}|, \\ (\hat{\gamma}\cdot\hat{\nu}) = \sin i_\xi\sin\delta\sin(\varphi-\varphi_S) - \cos\delta\cos i_\xi\,, \\ (\hat{\gamma}\cdot\dot{\boldsymbol{u}}_t) = [\sin i_\xi\cos\lambda\cos(\varphi-\varphi_S) - \sin i_\xi\sin\lambda\cos\delta\sin(\varphi-\varphi_S) - \cos i_\xi\sin\lambda\sin\delta]\,|\dot{\boldsymbol{u}}_t|, \\ (\hat{\nu}\cdot\hat{p}) = \sin\delta\cos i_\xi\sin(\varphi-\varphi_S) + \sin i_\xi\cos\delta, \\ (\dot{\boldsymbol{u}}_t\cdot\hat{p}) = [\cos i_\xi\cos\lambda\cos(\varphi-\varphi_S) + \cos i_\xi\cos\delta\sin\lambda\sin(\varphi-\varphi_S) + \sin i_\xi\sin\lambda\sin\delta]\,|\dot{\boldsymbol{u}}_t|, \\ (\hat{\nu}\cdot\hat{\varphi}) = \sin\delta\cos(\varphi-\varphi_S), \\ (\dot{\boldsymbol{u}}_t\cdot\hat{\varphi}) = -[\cos\lambda\sin(\varphi-\varphi_S) + \sin\lambda\cos\delta\cos(\varphi-\varphi_S)]\,|\dot{\boldsymbol{u}}_t|. \end{array}\right. \tag{18}$$

Substituting in the first of (11), in (12) and (13) we finally obtain the radiation patterns in terms of the unknowns u_t, u_n δ, λ, φ_S and in terms of φ, i_ξ which determine the direction of the ray indicating the elastic parameters with λ_1, μ_1.

$$
(19)\quad
\begin{cases}
\mathcal{F}^P = \{\cos\lambda\sin\delta\sin^2 i_\xi \sin 2(\varphi-\varphi_S) - \cos\lambda\cos\delta\sin 2 i_\xi \cos(\varphi-\varphi_S) + \\
\quad +\sin\lambda\sin 2\delta[\cos^2 i_\xi - \sin^2(\varphi-\varphi_S)\sin^2 i_\xi] + \\
\quad +\sin\lambda\cos 2\delta\sin 2 i_\xi \sin(\varphi-\varphi_S)\} |\dot{\boldsymbol{u}}_t|/|\dot{\boldsymbol{u}}| + \\
\quad + \dfrac{\lambda_1}{\mu_1} |\dot{\boldsymbol{u}}_n|/|\dot{\boldsymbol{u}}| + 2[\sin i_\xi \sin\delta\sin(\varphi-\varphi_S) - \cos\delta\cos i_\xi]^2 |\dot{\boldsymbol{u}}_n|/|\dot{\boldsymbol{u}}|, \\
\mathcal{F}^{SV} = \Big\{\sin\lambda\cos 2\delta\cos 2 i_\xi \sin(\varphi-\varphi_S) - \cos\lambda\cos\delta\cos 2 i_\xi \cos(\varphi-\varphi_S) + \\
\quad + \dfrac{1}{2}\cos\lambda\sin 2\delta\sin 2 i_\xi \sin 2(\varphi-\varphi_S) + \\
\quad - \dfrac{1}{2}\sin\lambda\sin 2\delta\sin 2 i_\xi [1+\sin^2(\varphi-\varphi_S)]\Big\} |\dot{\boldsymbol{u}}_t|/|\dot{\boldsymbol{u}}| + \\
\quad + \{\sin 2\delta\cos 2 i_\xi \sin(\varphi-\varphi_S) + \sin 2 i_\xi [\sin^2\delta\sin^2(\varphi-\varphi_S) - \cos^2\delta]\} |\dot{\boldsymbol{u}}_n|/|\dot{\boldsymbol{u}}|, \\
\mathcal{F}^{SH} = \Big[\cos\lambda\cos\delta\cos i_\xi \sin(\varphi-\varphi_S) + \cos\lambda\sin\delta\sin i_\xi \cos 2(\varphi-\varphi_S) + \\
\quad + \sin\lambda\cos 2\delta\cos i_\xi \cos(\varphi-\varphi_S) - \dfrac{1}{2}\sin\lambda\sin 2\delta\sin i_\xi \sin 2(\varphi-\varphi_S)\Big] |\dot{\boldsymbol{u}}_t|/|\dot{\boldsymbol{u}}| + \\
\quad + 2\sin^2\delta\cos^2(\varphi-\varphi_S) |\boldsymbol{u}_n|/|\boldsymbol{u}|.
\end{cases}
$$

In order to obtain intrinsic expressions of the radiation pattern we must now eliminate the size of the dislocation and retain only its direction; this is done by setting

$$
u_t = u\cos\vartheta, \qquad u_n = u\sin\vartheta,
$$

where ϑ is the angle between the dislocation and the fault plane. Substituting in (19) we finally find the expression of the radiation pattern as function of angular terms only:

$$
(20)\quad
\begin{cases}
\mathcal{F}^P = \{\cos\lambda\sin\delta\sin^2 i_\xi \sin 2(\varphi-\varphi_S) - \cos\lambda\cos\delta\sin 2 i_\xi \cos(\varphi-\varphi_S) + \\
\quad +\sin\lambda\sin 2\delta[\cos^2 i_\xi - \sin^2(\varphi-\varphi_S)\sin^2 i_\xi] + \\
\quad +\sin\lambda\cos 2\delta\sin 2 i_\xi \sin(\varphi-\varphi_S)\}\cos\vartheta + \\
\quad + \left\{\dfrac{\lambda_1}{\mu_1} + 2[\sin i_\xi \sin\delta\sin(\varphi-\varphi_S) - \cos\delta\cos i_\xi]^2\right\}\sin\vartheta, \\
\mathcal{F}^{SV} = \Big\{\sin\lambda\cos 2\delta\cos 2 i_\xi \sin(\varphi-\varphi_S) - \cos\lambda\cos\delta\cos 2 i_\xi \cos(\varphi-\varphi_S) + \\
\quad + \dfrac{1}{2}\cos\lambda\sin 2\delta\sin 2 i_\xi \sin 2(\varphi-\varphi_S) + \\
\quad - \dfrac{1}{2}\sin\lambda\sin 2\delta\sin 2 i_\xi [1+\sin^2(\varphi-\varphi_S)]\Big\}\cos\vartheta + \\
\quad + \{\sin 2\delta\cos 2 i_\xi \sin(\varphi-\varphi_S) + \sin 2 i_\xi [\sin^2\delta\sin^2(\varphi-\varphi_S) - \cos^2\delta]\}\sin\vartheta, \\
\mathcal{F}^{SH} = [\cos\lambda\cos\delta\cos i_\xi \sin(\varphi-\varphi_S) + \cos\lambda\sin\delta\sin i_\xi \cos 2(\varphi-\varphi_S) + \\
\quad + \sin\lambda\cos 2\delta\cos i_\xi \cos(\varphi-\varphi_S) - \dfrac{1}{2}\sin\lambda\sin\delta\sin i_\xi \sin 2(\varphi-\varphi_S)]\cos\vartheta + \\
\quad + 2\sin^2\delta\cos^2(\varphi-\varphi_S)\sin\vartheta.
\end{cases}
$$

The case of $\vartheta = 0$ obviously reproduces the pure slip source.

The solution of the inverse problem.

In order to solve the real problem we should now be able to obtain the parameters describing the source from the radiation pattern obtained from the recordings at the observing stations. In practical terms we must obtain ϑ, δ, λ, φ_S, u from the size and polarity of the signals observed at the stations recording the events. The retrieval of the size of u will dependent mostly on the calibration of the instruments and their sites, and on the attenuation on the ray paths; however, if the instruments are equal and the attenuation is isotropic (the latter not being always true) the method should allow the retrieving of the goemetric parameters of the source from the observed data, with an appropriate correction for the attenuation on the ray paths depending only on the distance from the source to the receiver.

We shall follow the method developed by Shapira and Bath (1978) for a pure shear source, supposing the linear size of the source to be small in comparison with the distance from the nearest station. The assumption of a point source allows the use of equations (20) only if the events to be studied are weak enough.

The method is based on displacement amplitudes of first P motion measured by vertical component seismometers of a small local network surrounding the source. Such amplitudes are compared with those computed iteratively changing the source parameters (ϑ, δ, λ, and φ_S) until the minimum discrepancy between the observed and computed amplitudes is reached.

The ray parameters φ and i_ξ for each station are easily found if the station and source coordinates are known and the crustal model in the concerned area is given. As remarked by Shapira and Bath (1977), the quality of both the hypocentral location and the fault parameter solution strongly depend on the use of an appropriate crust model.

Because of different incidence angles for rays to different stations, we must convert the vertical component amplitude into total amplitude. For free surface stations, reflected P and SV waves have to be considered and the vertical component amplitude must be corrected accordingly (Bath *et al.*, 1976). Moreover, all the observed amplitudes must also corrected for the goemetrical spreading depending on the hypocentral distance. Both corrections are expressiôn by

$$A_{mi} = D_i^m K(\gamma_i) A_{zi} \tag{21}$$

where A_{mi} is the corrected amplitude observed at the i-th station, D_i is the hypocentral distance, $K(\gamma_i)$ is the conversion factor between vertical and total amplitude, depending on the incidence angle γ_i, m is the spreading factor, and A_{zi} is the vertical component amplitude meausured on the recorded signal.

The corrected amplitudes A_{mi} are not yet comparable with the theoretical amplitude A_i computed by the radiation pattern given in equation (20).

The normalized amplitudes are defined as:

$$\hat{A}_{mi} = \frac{A_{mi}}{|A_{mk}|}; \qquad \hat{A}_i = \frac{A_i}{|A_k|}; \tag{22}$$

where $|A_{mk}|$ and $|A_k|$ are the maximum absolute values of all the measured and computed amplitudes respectively.

The best fit for the four source parameters is reached by minimizing the discrepancy between the theoretical and observed amplitudes. In order to accomplish it, we define the standard derivation

$$\sigma_A^2 = \frac{1}{N-1}\sum_i^N (\hat{A}_{mi} - \hat{A}_i)^2\,, \tag{23}$$

where N is the total number of stations. The solution is found for $\sigma_A^2 = \min$.

Among the many methods of minimization available in literature, we chose a very simple one which consists in the search for an approximate solution by scanning all the possible sets of parameters (ϑ, δ, λ, φ_S) by given steps in their total range from $-\pi/2$ to $\pi/2$. In the following iteration a new search for the minimum of (23) is performed, reducing both the steps and ranges around the approximate solution.

Testing the method.

A computer program based on the criteria described in the previous paragraph was written for the inversion of the source parameters (ϑ, δ, λ and φ_S) from vertical amplitudes of P waves recorded at a number of stations.

The reliability of the results obtained by the inversion programme should be confirmed by two kinds of tests:

— on the algorithms contained in the program, which must correspond to the theory from which they were derived, and the efficiency of the inversion process minimizing the residuals for the best fit;

— on the physical meaning of the method with respect to the particular experimental conditions under which it is used.

As far as the first point is concerned, we have prepared a «direct» program that, on the basis, of the expression of the radiation pattern given by (20) and the propagation effects given by (21), computes the theoretical amplitudes measurable at the stations of a seismometric network for a given source model (defined by the four angles ϑ, δ, λ and φ_S). By processing these synthetic data with the inversion program as they were read on real recordings, one must obtain source parameters identical to those used for their simulation. This test has shown that the inversion program can provide satisfactory results starting from a wide range of situations regarding the source parameters and station distributions.

As to the second kind of test, it has not yet been possible to carry out any direct check, because of the lack of experimental data to be used for this purpose. Instead, we studied the stability of the results when the input data (amplitudes) are affected by statistical errors, which simulate the actual data. The most critical point is whether a value of the parameter ϑ different from zero reflects a real discrepancy from a pure shear source, or whether it comes only from the obvious capacity of the four-parameters model to fit experimental data better than the three-parameters one.

In order to carry out our tests, we have prepared synthetic sets of data starting from a given model simulating real experimental environments. The source to be analysed was located at five kms depth, in the first layer of a two-layer crust. The data were supposed collected by a network of 12 stations, almost uniformly azimuthally

Table I. *Station and ray parameter.*

Station name	Δ (km)	φ (deg)	i_ξ (deg.)	Theoretical amplitudes A_i			
				($\vartheta = 0°$)	($\vartheta = 10°$)	($\vartheta = 20°$)	($\vartheta = 30°$)
sta1	10.0	318	116.5	0.017	0.216	0.150	0.129
sta2	9.4	8	118.1	0.596	1.000	0.455	0.315
sta3	12.4	26	56.4	− 0.204	0.004	0.097	0.114
sta4	8.3	283	121.0	0.029	0.286	0.196	0.167
sta5	3.3	124	146.8	− 0.873	0.814	1.000	1.000
sta6	9.2	216	118.6	− 0.112	0.110	0.133	0.132
sta7	9.3	180	118.4	− 0.600	− 0.402	− 0.016	0.071
sta8	8.7	129	119.8	− 1.000	− 0.678	− 0.032	0.113
sta9	13.4	65	56.4	0.056	0.257	0.162	0.135
st10	17.2	194	56.4	0.495	0.816	0.367	0.252
st11	19.0	168	56.4	0.331	0.559	0.256	0.177
st12	19.2	331	56.4	− 0.537	− 0.377	− 0.026	0.053

distributed around the source, and with epicentral distance ranging from 3 to 19 kms. In such circumstances, seven stations would receive direct waves, and five refracted waves, as first arrivals.

The source parameters were assigned as follows: $\delta = 30°$, $\lambda = 45°$, $\varphi_S = 15°$ with four different choices for $\vartheta(\vartheta = 0°, 10°, 20°$ and $30°)$. In the case of $\vartheta = 0°$, six stations would observe negative polarity and six would observe positive polarity for the first P wave pulse.

Running the «direct» program, we obtained a set of synthetic data for each of the four cases not affected by any experimental errors.

By means of a computer programme we modified the synthetic observation data randomly, as they were affected by experimental errors of given standard deviations. Using such modified amplitudes in input, the inversion programme gives, as expected, different results at each time, and in this way the stability of the method can be tested simulating various qualities of input data.

For each of the four sets of source parameters, we added to the normalized $\hat{A}_i$ random values with zero mean and the same standard deviation $\sigma = 0.01$ (one percent of the maximum amplitude). The standard deviation was then increased in five steps to 0.02, 0.05, 0.10, 0.20 and 0.50. For the inversion of the source parameters we used, besides the general version of the program with four free parameters, a special version with the parameter ϑ constrained to zero.

For each of the above cases, the test was run ten times and the results were analysed computing the averages of the source parameters so obtained, and their standard deviation. In total, each version of the programmes (with four and three free parameters respectively) was tested with 240 different sets input data.

Several comments can be made about the results. Before doing that, we want to remark that running the regression programmes (both with four and three free parameters) sometimes the iteration stopped in a secondary minimum of the residual function expressed by (23). It was approximately located at the point $\varphi_S = 65°$, $\delta = -70°$, $\lambda = -$

TABLE II. *Parameters retrieved by the inversion program* (synthetic-model: $\gamma_g = 15°$, $\delta = 30°$, $\lambda = 45°$).

		Four parameters (ϑ free)					Three parameters ($\vartheta = 0°$)			
ϑ	σ	$\widetilde{\varphi}_S$	$\widetilde{\delta}$	$\widetilde{\lambda}$	$\widetilde{\vartheta}$	$\widetilde{\sigma}_A^2$	$\widetilde{\varphi}_S$	$\widetilde{\delta}$	$\widetilde{\lambda}$	$\widetilde{\sigma}_A^2$
0	0.01	14.6	30.0	44.4	0.0	0.00016	14.7	30.0	44.7	0.00014
		0.49	—	0.66	—		0.46	—	0.90	
	0.02	15.2	29.8	45.3	0.0	0.00045	14.8	30.0	45.2	0.00047
		1.25	0.60	1.79	—		0.98	—	1.72	
	0.05	14.4	29.9	45.5	− 0.1	0.0029	15.4	30.0	46.6	0.0041
		2.8	1.36	4.6	0.3		2.4	—	3.9	
	0.10	12.0	32.9	42.9	− 0.7	0.0093	13.6	30.0	47.4	0.012
		5.7	4.5	13.2	2.2		4.4	—	8.9	
	0.20	10.4	33.5	35.6	− 0.4	0.033	14.6	35.5	42.5	0.039
		11.8	7.2	26.7	4.8		8.7	8.5	27.2	
	0.50	13.0	41.0	31.0	1.3	0.099	5.6	22.0	59.0	0.098
		18.6	12.8	55.0	5.6		36.0	25.6	18.0	
10	0.01	15.0	30.0	44.9	10.0	0.00010	0.7	30.0	59.3	0.068
		0.45	—	0.45	—		0.64	—	0.64	
	0.02	14.9	30.1	44.7	10.0	0.00031	0.5	30.0	58.8	0.068
		1.04	0.30	1.10	—	1.02	—	0.74		
	0.05	16.0	29.8	46.1	10.0	0.0028	0.7	30.0	59.2	0.069
		1.95	1.33	3.3	0.63		2.1	—	1.4	
	0.10	13.5	30.6	41.9	10.1	0.0061	− 0.3	30.0	59.3	0.072
		4.1	2.4	4.9	0.87		3.5	—	3.1	
	0.20	8.9	31.8	32.6	10.7	0.022	3.3	30.0	64.3	0.090
		11.5	6.5	20.3	1.95		7.5	—	3.9	

TABLE II. – (*Continued*

		Four parameters (ϑ free)					Three parameters ($\vartheta = 0°$)			
ϑ	σ	$\tilde{\varphi}_S$	$\tilde{\delta}$	$\tilde{\lambda}$	$\tilde{\vartheta}$	$\tilde{\sigma}_A^2$	$\tilde{\varphi}_S$	$\tilde{\delta}$	$\tilde{\lambda}$	$\tilde{\sigma}_A^2$
	0.50	– 7.0	38.4	24.0	9.0	0.071	11.1	27.8	66.2	0.127
		16.2	13.0	35.8	4.2		36.7	14.7	15.3	
20	0.01	12.3	30.1	37.0	21.2	0.00083	– 7.4	30.0	73.6	0.188
		3.2	0.70	8.6	1.47		0.66	—	0.49	
	0.02	12.7	30.4	41.0	20.8	0.0018	– 7.2	30.0	73.9	0.193
		4.5	1.36	5.5	1.47		0.92	—	0.74	
	0.05	14.0	32.1	38.7	20.8	0.0106	– 6.4	30.0	74.3	0.195
		7.9	6.1	12.3	2.1		2.4	—	2.6	
	0.10	3.4	36.6	27.4	20.4	0.022	– 3.9	30.0	75.9	0.187
		13.7	7.2	15.2	4.8		5.8	—	1.8	
	0.20	10.7	41.9	15.2	18.0	0.060	– 12.2	14.0	20.5	0.231
		11.7	15.5	31.8	4.5		40.4	52.0	51.1	
	0.50	13.2	– 15.9	– 17.5	10.8	0.134	– 5.9	– 18.0	– 14.7	0.268
		40.8	53.1	52.9	4.4		45.6	63.4	38.5	
30	0.01	15.3	29.9	44.5	29.8	0.00069	2.5	– 60.0	– 73.3	0.286
		1.68	0.83	4.1	1.7		1.02	—	1.10	
	0.02	14.2	30.4	45.4	30.1	0.0030	2.0	60.0	– 73.3	0.306
		5.3	1.9	4.3	1.81		1.73	—	1.79	
	0.05	12.3	34.0	32.9	29.5	0.016	0.14	– 60.0	– 74.3	0.281
		7.4	9.8	19.7	3.5		1.12	—	1.03	
	0.10	12.5	45.0	27.1	26.0	0.038	– 4.3	– 24.4	– 41.7	0.264
		23.7	13.7	24.2	6.0		7.9	34.6	72.0	
	0.20	16.3	33.1	34.9	19.5	0.101	7.6	– 10.0	– 1.9	0.273
		5.7	37.6	65.9	8.2		12.4	47.8	76.4	
	0.50	14.5	7.1	6.9	8.8	0.272	– 8.8	42.0	41.5	0.217
		36.4	56.2	54.4	9.9		40.3	38.1	53.3	

$-70°$. All these anomalous solution were discarded from the subsequent analysis. It must be noted, however, that even in these peculiar circumstances, the inversion program could provide a solution with a value of ϑ very close to that put in the model used by the direct program.

First of all, we note that the method provides excellent results in all the cases with $\sigma = 0.01$ and $\sigma = 0.02$, when the algorithm with four free parameters is used. The results are also very good for $\sigma = 0.05$ and $\vartheta \leqslant 10°$, and are still rather reliable for $\vartheta \geqslant 20°$. The standard deviation of the solution increases, in general, with the increase of the standard deviation of the input data, but the parameter ϑ appears to be the least sensitive to the variation of the quality of data. The fact that the parameter δ is the most stable and the parameter λ is the most unstable of the other three parameters could be concerned with our particular choice of the source model in connection with the geometrical distribution of the stations.

The average values of the residual variance σ_A^2 are, in all cases, increasing proportionally to the variance of the input data.

When the parameter ϑ is constrained to zero, on the contrary, there are good solution only if the source model is characterized by $\vartheta = 0°$ also. In the latter case, of course, there is not relevant difference with the results obtained by the four free parameters algorithm. As far as we increase the value of ϑ, therefore increasing the intensity of the crack opening, the solution becomes more and more disturbed in the other three parameters, that are typical of a pure shear source.

From the above results it can be inferred that we can not expect good results from a focal mechanism solution modelling the source as a pure sear type, if we are actually in the presence of a not negligible component of the displacement vector normal to the fault. In this case the values of the residual variance σ_A^2 are always rather high and do not depend very much on the standard deviation of the input amplitudes.

Increasing σ to 0.10, we still obtain fairly good results using the programme of the general model with four free parameters. The standard deviation of the parameter ϑ is of the order of magnitude of a few degrees. The values obtained of λ seem to be, at least in our case, the least reliable.

Moving to $\sigma = 0.20$, the results are stable only for the parameter ϑ, which exhibits a standard deviation of a few degrees only. The parameters φ_S and δ seem to be still fairly reliable if $\vartheta \leqslant 20°$, but λ is almost meaningless.

The case of $\sigma = 0.50$ brings us to the completely random behaviour for the results concerning the three «pure shear» parameters φ_S, δ and λ. Nevertheless, the values of ϑ are still consistent with those of the given model at least for $\vartheta \leqslant 10°$, and affected by a standard deviation not exceending 10° even in the worst case. A systematic reduction is noted in the values of c for the results of the inversion program with respect to those of the source model for $\vartheta \geqslant 20°$. However, we can note that the average value of the residual function σ_A^2 obtained running the inversion programme with four parameters for $\vartheta \geqslant 10°$, even in the case of $\sigma = 0.50$, is less than the corresponding values obtained by the program with ϑ constrained to zero, and no errors on the input data.

References

Aki K. and P. Richards (1980) – *Quantitative Seismology*, W. H. Freeman and Co., San Francisco,

De Natale G. and A. Zollo (1986) – *Parametri di sorgente sismica e caratteristiche del mezzo di propagazione ai Campi Flegrei dedotti dall'analisi di dati da una rete sismica digitale a 3 componenti*, Convegno del Gruppo Nazionale per la Geofisica della Terra Solida, CNR. Roma.

Furomoto M. and Y. Fukao (1976) – *Seismic moments of great deep shocks*, «Phys. Earth Plan Int.», 11, 352-357.

Gilbert F. (1971) – *Excitation of the normal modes of the Earth by earthquake source*, «Geophys. J. R. Astr. Soc.», 22, 223-226.

Gilbert F.and A. Dziewonsky (1975) – *An application of normal mode theory to the retrieval of structural parameters and source mechanism from seismic spectra*, «Phil. Trans. R. Soc. London, Ser. A», 278, 187-269.

Julian B. R. and S. A. Sipkin (1985) – *Earthquake processes in the Long Valley caldera area, California*, «J. Geoph. Res.», 90, 11, 155-11, 169.

McCowan D. (1976) – *Moment tensor representation of surface waves sources*, «Geophys. J. R. Astr. Soc.», 44, 595-599.

Mendiguren I (1977) – *Source mechanism of a deep earthquake from analysis of world wide observations of free oscillations*, Ph. D. Thesis, Massachusset Institute of Technology, Cambridge, Ma.

Shapira A. and M. Bath (1977) – *Short distance hypocentral location in layered media*, Seismological Institute, Uppsala, Report no. 2-77.

Shapira A. and M. Bath (1978) – *Source mechanism determination of short distance microearthquakes*, Seismology Institute, Uppsala, Report no. 1-78.

Strelitz R. A. (1980) – *The fate of the downgoing slab: a study of the moment tensor from body waves of complex deep-focus earthquakes*, «Phys. Eerth Plan. Int.», 21, 83-96.

Stump B. W. (1976) – *The determination of source mecanism studies*, «Trans. Am. Geophys. Un.», 57, 953.